Submitted to Physical Review

RECEIVED
LAWRENCE
RADIATION LABORATORY
DEC 5 1969
LIBRARY AND
DOCUMENTS SECTION

UCRL-19302
Preprint

Cy. 2

SEARCH FOR AN ELECTRON MASS SHIFT IN ^{133}Cs IN AN INTENSE ELECTROMAGNETIC FIELD

J. Richard Mowat, Charles E. Johnson, and Howard A. Shugart and Vernon J. Ehlers

September 5, 1969

AEC Contract No. W-7405-eng-48

TWO-WEEK LOAN COPY

This is a Library Circulating Copy which may be borrowed for two weeks. For a personal retention copy, call Tech. Info. Division, Ext. 5545

LAWRENCE RADIATION LABORATORY
UNIVERSITY of CALIFORNIA BERKELEY

UCRL-19302

Cy. 2

DISCLAIMER

This document was prepared as an account of work sponsored by the United States Government. While this document is believed to contain correct information, neither the United States Government nor any agency thereof, nor the Regents of the University of California, nor any of their employees, makes any warranty, express or implied, or assumes any legal responsibility for the accuracy, completeness, or usefulness of any information, apparatus, product, or process disclosed, or represents that its use would not infringe privately owned rights. Reference herein to any specific commercial product, process, or service by its trade name, trademark, manufacturer, or otherwise, does not necessarily constitute or imply its endorsement, recommendation, or favoring by the United States Government or any agency thereof, or the Regents of the University of California. The views and opinions of authors expressed herein do not necessarily state or reflect those of the United States Government or any agency thereof or the Regents of the University of California.

Submitted to the Physical Review UCRL-19302

SEARCH FOR AN ELECTRON MASS SHIFT IN ^{133}Cs IN AN INTENSE ELECTROMAGNETIC FIELD*

J. Richard Mowat†, Charles E. Johnson, and Howard A. Shugart
Department of Physics and Lawrence Radiation Laboratory
University of California, Berkeley, California

and

Vernon J. Ehlers

Department of Physics, Calvin College, Grand Rapids, Michigan

September 5, 1969

ABSTRACT

The possibility that the mass of a bound electron changes when placed in an intense electromagnetic field is studied here both theoretically and experimentally. The atomic-beam magnetic-resonance technique was used to examine hyperfine-structure frequency shifts in ^{133}Cs that occur when the atom is subjected to an intense, non-resonant radio-frequency magnetic field perpendicular to the static "C" field. A 2921-MHz TM_{010} cavity produced the perturbing field and was situated between Ramsey separated oscillatory loops, which induced the resonant transitions of interest. Shifts were observed for six $\Delta m_F = \pm 1$ transitions at field-independent points. No evidence was found for an electron mass shift. Good agreement is found between all observed shifts and those expected from a multi-level Bloch-Siegert effect. Theoretical arguments, based upon perturbation theory, are given explaining why the mass-shift effect does not occur in the ground state hyperfine structure of a hydrogen-like system.

I. INTRODUCTION

It has been suggested[1] that, when an electron interacts with a classical, plane polarized electromagnetic field, a finite mass renormalization occurs such that the electron's observable mass increases, becoming

$$m_* = \left[m_o^{\,2} + \left(\frac{ea}{c^2}\right)^2\right]^{\frac{1}{2}} \simeq m_o + \frac{1}{2}\frac{e^2a^2}{m_oc^4} \tag{1}$$

where m_o is the electron rest mass in the absence of the field, e is the electron charge, c is the speed of light in vacuum, and a is the (real) scalar amplitude of the vector potential describing the field. The relative mass shift is defined by

$$\frac{m_* - m_o}{m_o} \equiv \frac{\delta m}{m} \simeq \frac{1}{2}\frac{e^2a^2}{(m_oc^2)^2} \quad .$$

Sengupta[2] in 1952 first suggested the possibility that the mass of a free electron might be observed to increase when the electron is allowed to interact with an intense electromagnetic field. This mass-shift effect is just one of many interesting and controversial predictions of theories of intense-field electrodynamics that have appeared over the past few years. Sarachik[3] has recently made a comprehensive survey of these effects, none of which have yet been observed experimentally owing to the difficulty in generating sufficiently intense laser fields.

In 1966 Reiss[4] suggested that an intensity-dependent mass shift could be observed for a bound electron in a plane-wave radio-frequency

field. He pointed out that an electron mass increase would affect precision measurements made of spectral lines from a hydrogen-like system. Such spectral lines depend on the electron mass through the Rydberg energy $Ry = -\frac{1}{2}\alpha^2 mc^2$ and the Bohr magneton $\mu_o = \frac{e\hbar}{2mc}$.

The mass-shift hypothesis for an electron bound in the ground state of a hydrogen-like system is examined here both theoretically and experimentally. It is found that, if all the effects of the plane wave field are treated in a consistent manner using perturbation theory, then the mass-shift effect is not expected. In addition, experimental work of sufficient sensitivity to observe the mass-shift effect has yielded negative results.[5]

II. THEORY OF THE POSTULATED ELECTROMAGNETIC MASS SHIFT

The following discussion is similar to the one outlined by Reiss[4] for the hydrogen atom, but it is more detailed because it does not neglect effects due to the electron spin. A non-relativistic wave equation is obtained for hydrogen-like atoms which displays the mass-shift effect explicitly up to and including the Zeeman energy and spin-orbit coupling terms. Perturbation theory is then applied to the ground state eigenfunction of the approximate Hamiltonian, and the usual Fermi formula for the hyperfine structure (hfs) splitting is obtained, and it also displays the mass shift. Finally, an examination is made of the dependence of the ground state hfs Zeeman levels on the electron mass.

A. Origin of the Mass Shift Hypothesis

The interaction of a spin 1/2 particle with external electric ($\vec{E}$) and magnetic ($\vec{B}$) fields can be described by the following equation:

$$(E - e\phi)^2\psi = [c^2(\vec{p} - \frac{e}{c}\vec{A})^2 + (mc^2)^2 - e\hbar(\vec{\sigma}\cdot\vec{B} - i\vec{\alpha}\cdot\vec{E})]\psi \qquad (2)$$

where $\vec{B} = \nabla \times \vec{A}$ and $\vec{E} = -\frac{1}{c}\frac{\partial\vec{A}}{\partial t} - \nabla\phi$ are derived from the magnetic vector potential $\vec{A}$ and the electrostatic scalar potential ϕ. $E = i\hbar\frac{\partial}{\partial t}$ and $\vec{p} = -i\hbar\nabla$ are the total energy and momentum operators, respectively. The Dirac matrix $\vec{\alpha}$ is defined by

$$\vec{\alpha} = \begin{pmatrix} 0 & \vec{\sigma} \\ \vec{\sigma} & 0 \end{pmatrix} \quad ;$$

$\vec{\sigma}$ is a vector comprising the three Pauli matrices, and ψ is a four-component spinor wave function.

Consider the following vector potential:

$$\vec{A} = \vec{A}_{rot} + \vec{A}_s \tag{3}$$

where

$$\vec{A}_{rot} = a \text{ Re } [(\hat{y} \pm i\hat{z}) \, e^{-i(\omega t - kx)}]$$

is the vector potential of a circularly polarized plane wave of angular frequency ω and wave number k propagating in the +x direction with velocity $c = \frac{\omega}{k}$ and amplitude a, and

$$\vec{A}_s = - B_o \, y \, \hat{x}$$

is the vector potential of a uniform, static magnetic field, $\vec{B}_s = B_o \, \hat{z}$. When Eq. (3) is substituted into Eq. (2), one obtains

$$(E - e\phi)^2 \psi = \Big[c^2 (\vec{p} - \frac{e}{c} \vec{A}_s)^2 + (mc^2)^2 + e^2 A_{rot}^2 - e\hbar(\vec{\sigma} \cdot \vec{B}_s - i\vec{\alpha} \cdot \vec{E}_s)$$
$$- 2ec \, \vec{A}_{rot} \cdot \vec{p} - e\hbar(\vec{\sigma} \cdot \vec{B}_{rot} - i\vec{\alpha} \cdot \vec{E}_{rot}) \Big] \psi \tag{4}$$

where the subscripts "rot" and "s" refer to the plane wave field and the static fields, respectively. In order to keep the wave equation time-independent, the last three terms in Eq. (4) will be temporarily ignored and considered later in Section II-D. For the frequencies of interest, the two terms involving $\vec{B}_{rot}$ and $\vec{E}_{rot}$ are of small magnitude compared to the $e^2 A_{rot}^2$ term and also compared to the static terms containing $\vec{B}_s$ and $\vec{E}_s$ (Zeeman effect and spin-orbit coupling). These two time-dependent terms can be satisfactorily accounted for through the use of time-dependent perturbation theory. The $\vec{A}_{rot} \cdot \vec{p}$ term, on the other hand, will be shown to be of the same order as the $e^2 A_{rot}^2$ term.

Once the time dependence in Eq. (4) has been removed, the time variation of ψ can be separated out, and the operator E can be replaced by the total energy, also designated E. For circular polarization,

$$e^2A^2_{rot} = e^2\,\vec{A}_{rot}\cdot\vec{A}_{rot} = e^2a^2 \quad .$$

Since e^2a^2, like $(mc^2)^2$, is a constant scalar, it was suggested by Reiss[1] that the e^2a^2 term serves as a finite mass renormalization, and that one should define an effective mass m_* by

$$(m_*c^2)^2 = (mc^2)^2 + e^2a^2 \quad .$$

As a first step toward obtaining a non-relativistic wave equation from Eq. (4), we can transfer the $(m_*c^2)^2$ term to the left-hand side, divide by $2m_*c^2$, drop the subscripts s, and introduce the definition

$$W = E - m_*c^2 \tag{5}$$

so the wave equation can be put into the form

$$\left[\frac{1}{2m_*}\left(\vec{p} - \frac{e}{c}\vec{A}\right)^2 + e\phi - \frac{e\hbar}{2m_*c}\left(\vec{\sigma}\cdot\vec{B} - i\vec{\alpha}\cdot\vec{E}\right) - \frac{1}{2m_*c^2}\left(W - e\phi\right)^2\right]\psi = W\psi. \tag{6}$$

This equation is the same as the one given by Bethe and Salpeter[6] for an electron in an external, static field, except that the electron mass has everywhere been replaced by m_*, the renormalized mass given by Eq. (1).

B. The Non-Relativistic Wave Equation

Equation (6) can be transformed, in the spirit of the Foldy-Wouthuysen method, to obtain a non-relativistic wave equation which contains Zeeman energy and spin-orbit coupling terms which are the same as in the usual non-relativistic theory except that the electron mass is everywhere replaced by the renormalized mass m_*. The approximation is

good only to order $1/m^2$ so the last term in Eq. (6) which is of order $1/m^3$ is neglected. Hence the starting point for a reduction to a non-relativistic wave equation is the following:

$$\mathcal{H}_o \psi_o = W\psi_o$$

where

$$\mathcal{H}_o = \frac{1}{2m_*} (\vec{p} - \frac{e}{c}\vec{A})^2 + e\phi - \frac{e\hbar}{2m_*c}\vec{\sigma}\cdot\vec{B} + \frac{ie\hbar}{2m_*c}\vec{\alpha}\cdot\vec{E} \quad .$$

The following unitary transformation is introduced:

$$\mathcal{H}_{nr} = e^u \mathcal{H}_o e^{-u}$$

$$\psi_{nr} = e^u \psi_o$$

where

$$u = \frac{1}{2m_*c}\vec{\alpha}\cdot(\vec{p} - \frac{e}{c}\vec{A})$$

and $\mathcal{H}_{nr}$ is the non-relativistic Hamiltonian. The unitarity of the transformation can be established by using the identity

$$e^A B e^{-A} = B + [A,B] + \frac{1}{2!}[A,[A,B]] + \frac{1}{3!}[A,[A,[A,B]]] + \cdots \quad .$$

After a lengthy but straightforward calculation one obtains

$$\mathcal{H}_{nr}\psi_{nr} = E\psi_{nr}$$

where

$$\mathcal{H}_{nr} = m_*c^2 + \frac{1}{2m_*}(\vec{p} - \frac{e}{c}\vec{A})^2 + e\phi - \frac{e\hbar}{2m_*c}\vec{\sigma}\cdot\vec{B} + \frac{e\hbar}{2m_*c}\frac{\vec{\sigma}}{2}\cdot\frac{\vec{E}}{m_*c}\times(\vec{p} - \frac{e}{c}\vec{A})$$
$$- \frac{1}{4}\frac{e\hbar}{2m_*c}\vec{\sigma}\cdot\frac{\vec{p}\times\vec{E}}{m_*c} + \frac{e}{8}(\frac{\hbar}{m_*c})^2\nabla\cdot\vec{E} \quad . \qquad (7)$$

This Hamiltonian, except for the replacement of m by m_*, is identical in form to the approximate Hamiltonian obtained when the Foldy-Wouthuysen transformation is applied twice to the linear Dirac equation[7] for an electron in static electric and magnetic fields.

C. Application to Hyperfine Structure

It has just been shown that when time-dependent terms can be neglected, the sole effect of the plane wave field is to change the electron mass from m to m_* everywhere that it appears in the non-relativistic Hamiltonian; thus, Eq. (7) displays the mass-shift effect in the Zeeman energy and in the spin-orbit coupling terms. In particular, the Bohr magneton changes by just the amount expected due to an electron mass shift.

Presumably, the eigenfunctions and eigenvalues of $\mathcal{H}_{nr}$ are the same as in the absence of the plane wave except that the electron rest mass should be replaced everywhere it appears by the renormalized mass m_*. One consequence of this result is that perturbation theory applied to the usual correction terms gives the same energy splittings except for the mass change. The static perturbation of the $^2S_{1/2}$ hydrogen ground state due to the interaction of the electronic and nuclear spins leads to the usual Fermi formula for the hyperfine structure separation ΔW, with the electron mass replaced by m_*. A nucleus possessing a static magnetic dipole moment $\vec{\mu}_I$ produces a zero-field hfs splitting of the $^2S_{1/2}$ ground state given by

$$\Delta W = \frac{8\pi}{3} \frac{2I + 1}{I} \mu_e \mu_I |\psi_o(0)|^2 \quad . \tag{8}$$

The interaction of the electronic and nuclear magnetic dipole moments with an external static magnetic field H_o further splits the $|F\ m_F\rangle$ states. The application of degenerate perturbation theory leads to the Breit-Rabi formula[8] for the energy E of the state $|F\ m_F\rangle$ as a function of applied field H_o:

$$E = -\frac{\Delta W}{2(2I+1)} - \frac{\mu_I}{I} H_o\, m_F \pm \frac{\Delta W}{2}\left[1 + \frac{4m_F}{2I+1}x + x^2\right]^{1/2}$$

where

$$x \equiv \left(\frac{\mu_I}{I} - \frac{\mu_e}{S}\right)\frac{H_o}{\Delta W}$$

is the magnetic field parameter.

The change in the hfs energy levels due to a change in the electron mass can be obtained by differentiating the Breit-Rabi formula with respect to the electron mass. The hydrogenic wave function can be used to evaluate $|\psi_o(0)|^2$ in the Fermi formula so that the explicit mass dependence of ΔW can be ascertained. Using $|\psi_o(0)|^2 = \frac{1}{\pi}(Ze^2)^3\, m_*^2/\hbar^6$ and $\mu_e = \frac{e\hbar}{2m_*c}$, one finds, with $m_* \simeq m$,

$$\Delta W \propto m^2$$

and

$$\delta(\Delta W) = 2\,\frac{\delta m}{m}\,\Delta W \quad , \tag{9}$$

where $\frac{\delta m}{m}$ is the electron's relative mass shift. In the same fashion one can write

$$x = \frac{\mu_I}{I}\frac{H_o}{\Delta W} - \frac{\mu_e}{S}\frac{H_o}{\Delta W} \propto c_1 m^{-2} + c_2 m^{-3}$$

where c_1 and c_2 do not depend upon m. The change in x due to a

change in m is

$$\delta x = \frac{\delta m}{m} \frac{H_o}{\Delta W} \left(- \frac{2\mu_I}{I} + \frac{3\mu_e}{S} \right) .$$

With these results for $\delta(\Delta W)$ and δx, one obtains, after a straightforward differentiation of the Breit-Rabi formula,

$$\delta E = \frac{\delta m}{m} \left[- \frac{\Delta W}{2I + 1} \pm \Delta W \, R \pm \frac{H_o}{2R} \left(- \frac{2\mu_I}{I} + \frac{3\mu_e}{S} \right) \left(\frac{2m_F}{2I + 1} + x \right) \right]$$

where

$$R = \left(1 + \frac{4m_F}{2I + 1} x + x^2 \right)^{\frac{1}{2}} .$$

This equation gives the change in energy of the hfs level $|F \, m_F\rangle$ due to a relative change $\frac{\delta m}{m}$ in the mass of the electron. This shift is not the same for all hyperfine levels as indicated by the dependence of δE on m_F and F, i.e., through the ± sign. The frequency shift for a transition between levels of energy E_1 and E_2 due to a shift in the electron mass is given by

$$\delta f = \frac{\delta E_1 - \delta E_2}{h} \propto \frac{\delta m}{m} .$$

Hence the shift of a transition frequency is proportional to the relative mass shift. For most cases of experimental interest, a relative mass shift of, say, 10^{-6} results in a relative transition frequency shift of the same magnitude.

D. Consideration of Time-Dependent Terms

In the previous sections, a time-independent Hamiltonian whose eigenfunctions would be stationary states was obtained by neglecting the following three terms:

$$\mathcal{H}_{rot} = - \frac{e}{m_* c} \vec{A}_{rot} \cdot \vec{p} - \frac{e\hbar}{2m_* c} (\vec{\sigma} \cdot \vec{B}_{rot} - i\vec{\alpha} \cdot \vec{E}_{rot}) .$$

Any time-dependent perturbation can be broken up into its Fourier components, each of which can be studied separately. A typical component may be written in the form

$$\hbar b = Ve^{-i\omega t}, \; V \neq V(t) \quad .$$

The resulting transition probabilities, mixing parameters, and energy level shifts are proportional to the matrix elements of V between stationary states. The following discussion can therefore be simplified by dropping the factor $e^{-i\omega t}$ from $\vec{A}_{rot}$, $\vec{B}_{rot}$, and $\vec{E}_{rot}$.

For a circularly polarized plane wave, $\vec{E} = \pm i\vec{B}$; therefore the last two terms can be written, dropping the subscript "rot",

$$\frac{e\hbar}{2m_* c}(\vec{\sigma}\cdot\vec{B} - i\vec{\alpha}\cdot\vec{E}) = \frac{e\hbar}{2m_* c}(\vec{\sigma}\cdot\vec{B} \pm \vec{\alpha}\cdot\vec{B}) = \vec{\mu}_e\cdot\vec{B}\begin{pmatrix} I & \pm I \\ \pm I & I \end{pmatrix} \quad .$$

When B is one gauss, $\vec{\mu}_e\cdot\vec{B} \simeq 6 \times 10^{-9}$eV, and this term is much smaller than the hfs separation $\Delta W \simeq 6 \times 10^{-6}$eV. The treatment of such a term by time-dependent perturbation theory yields transition probabilities[9] for magnetic dipole transitions when ω is near a transition frequency and small frequency shifts[10] (Bloch-Siegert effect) when it is not. These frequency shifts are more than two orders of magnitude smaller than possible frequency shifts due to the postulated electron mass shift. It can be shown that this Zeeman energy term will be small compared to the mass renormalization term whenever $ea \gg \hbar\omega$.

For a circularly polarized plane wave where $\hat{\varepsilon} = \hat{y} \pm i\hat{z}$ and $\vec{k} = k\hat{x}$, the vector potential can be written

$$\vec{A}_{rot} = a\mathrm{Re}(\hat{\varepsilon}e^{i\vec{k}\cdot\vec{r}}) = a(\hat{y} \mp \hat{z}kx + \cdots) \quad .$$

The first-order correction to the ground state energy due to the interaction $\frac{-e}{m_* c}\vec{A}\cdot\vec{p}$ is

$$E_o^{(1)} = \langle n'|\frac{-e}{m_* c}\vec{A}\cdot\vec{p}|n\rangle \simeq -\frac{ea}{m_* c}\{\langle n'|p_y|n\rangle \mp k\langle n'|xp_z|n\rangle\} \tag{10}$$

where $|n\rangle$ stands for $|njIFm_F\rangle$ which is an hfs sublevel of the $|nj\rangle$ eigenstate. In first order perturbation theory, only the ground state sublevels need be considered. With the aid of the identities[11]

$$\langle m|\vec{p}|n\rangle = im_*\omega_{mn}\langle m|\vec{r}|n\rangle \tag{11}$$

$$\left.\begin{aligned}\langle m|r_i p_j|n\rangle &= \frac{1}{2}\, im_*\omega_{mn}\langle m|r_i r_j|n\rangle + \frac{1}{2}\langle m|L_k|n\rangle \\ \langle m|r_i p_i|n\rangle &= \frac{1}{2}\, im_*\omega_{mn}\langle m|r_i^2|n\rangle + \frac{1}{2}\, i\hbar\delta_{mn}\end{aligned}\right\} \tag{12}$$

where

$$\omega_{mn} = (E_m - E_n)/\hbar \quad ,$$

the first term in Eq. (10) becomes a matrix element of the position operator between two hfs levels. Such a matrix element must vanish because the ground state hfs levels all have the same parity. An application of Eq. (12) converts the second term into the matrix element of xz. This is essentially an electric quadrupole matrix element which vanishes in the case of a $^2S_{1/2}$ ground state because there can be no electric quadrupole interaction within a J = 1/2 state.

The second-order correction to the ground state energy due to the interaction $-\frac{ea}{m_* c}p_y$ is

$$E_o^{(2)} = \left(\frac{ea}{m_* c}\right)^2 \sum_{n\neq 0} \frac{\langle 0|p_y|n\rangle\langle n|p_y|0\rangle}{E_o^{(0)} - E_n^{(0)}}$$

where $|0\rangle$ represents any of the ground state hfs levels whose unperturbed energy is $E_o^{(0)}$, and $|n\rangle$ represents any hfs level of any other state. By the use of Eq. (11) this energy correction may be written as

$$E_o^{(2)} = \frac{e^2a^2}{m_*c^2}\frac{i}{\hbar}\sum_{n\neq 0}\langle 0|y|n\rangle\langle n|p_y|0\rangle \quad ,$$

which becomes, upon application of closure,

$$E_o^{(2)} = \frac{ie^2a^2}{\hbar m_*c^2}\{\langle 0|yp_y|0\rangle - \langle 0|y|0\rangle\langle 0|p_y|0\rangle\} \quad .$$

The second term in brackets vanishes as a result of the parity selection rule. With the aid of Eq. (12) the first term in the brackets is just $1/2\ i\hbar$; hence

$$E_o^{(2)} = -\frac{e^2a^2}{2m_*c^2} \quad . \tag{13}$$

Now, if the e^2A^2 term in Eq. (4) were retained, instead of being used to renormalize the mass, it would persist through the transformation of Section B above and appear in the resulting non-relativistic Hamiltonian as $e^2a^2/2mc^2$. Also, when the mass renormalization is not made, Eq. (13) reads $-e^2a^2/2mc^2$. Hence, the $\vec{A}\cdot\vec{p}$ term, taken to second order, exactly cancels the e^2A^2 term, taken to first order. These arguments based upon perturbation theory do not necessarily invalidate the mass-shift hypothesis. When, for example, the relative mass shift has the experimentally realizable value $\frac{\delta m}{m} = 2 \times 10^{-6}$, then

$$\frac{e^2a^2}{2mc^2} = \frac{e^2a^2}{2(mc^2)^2}mc^2 = \frac{\delta m}{m}mc^2 = 1 \text{ eV} \quad ,$$

which is certainly not small compared even to the gross structure. It

is therefore not clear that perturbation theory is the proper method for handling these terms.

III. DESCRIPTION OF THE EXPERIMENT

A. Experimental System

The atomic-beam magnetic-resonance technique was used in this search for an electron mass-shift effect in ^{133}Cs. Although the theory of the electron mass shift was developed in Section II with the hydrogen atom in mind, it should apply to alkali atoms whenever the valence electron experiences an electrostatic potential which is a function of radial position only (central field approximation). The non-central magnetic dipole interaction has already been accounted for by perturbation theory and has led to the hyperfine interaction described by the Fermi formula. The spherical symmetry of the $^2S_{1/2}$ electronic state forbids the existence of any multipole interactions beyond electric monopole and magnetic dipole.

Breit [12] and Kopfermann[13] have summarized some of the correction factors which should be applied to the Fermi formula before it is used to deduce alkali nuclear magnetic dipole moments from measured hyperfine energy separations. When these correction factors are taken into consideration, one obtains

$$\delta(\Delta W) = 1.96 \frac{\delta m}{m} \Delta W$$

which differs by only 2% from the result obtained in Eq. (9) assuming hydrogenic wave functions and no corrections to the Fermi formula.

The nuclear spin angular momentum I of ^{133}Cs is 7/2 $\hbar$ and the total electronic angular momentum in the ground state is $J = S = 1/2\ \hbar$. The total angular momentum $\vec{F} = \vec{I} + \vec{J}$ can assume in this case only the values $F = I + J = 4$ and $F = I - J = 3$. The projection of the total

angular momentum onto a preferred direction in space is given by the magnetic quantum number $m_F = F, F - 1, \cdots, -(F - 1), -F$. Figure 1, which is a plot of the Breit-Rabi formula in frequency units, shows how these levels are split by a static, externally applied magnetic field H_o. Effects of field inhomogeneities can be minimized by working at fields where the transition frequencies are only weakly dependent upon H_o. At those magnetic fields where $df/dH_o = 0$ (field-independent points), the transition frequency f is independent, to first order, of magnetic field H_o. Table I is a list of the field-independent $\Delta F = \pm 1$ transitions for ^{133}Cs. Four are of the σ type ($\Delta m_F = 0$), while six are of the π type ($\Delta m_F = \pm 1$). The six π transitions occur in three doublets which are labelled a, b, and c in Fig. 1. These three doublets were chosen for extensive study in the search for an electron mass shift.

B. Apparatus

A standard flop-in atomic-beam magnetic-resonance apparatus[14] utilizing the separated-oscillatory-field technique[15] is used to investigate shifts of hfs transition frequencies that occur as a cesium beam traverses a microwave cavity. Cesium atoms are produced in a resistance-heated steel oven by the reaction of calcium metal with a cesium halide, e.g.,

$$Ca + 2CsCl + heat \rightarrow CaCl_2 + 2Cs \quad .$$

1. Cavity-Hairpin Assembly. The actual experiment is performed in the constant-field region where appropriate resonant and non-resonant oscillating fields are introduced through the cavity-hairpin assembly.

Figure 2 is a sketch of the assembly with the cover removed to show the inside of the cavity. The beam passes from left to right, and the static field H_o is at right angles to the cavity faces. The entrance and exit apertures in the cavity each consist of four 0.055-inch diameter holes which serve to collimate the beam.

The cavity is resonant at 2.921 GHz (TM_{010} mode), and has an unloaded Q of 4200 ± 200 (determined by a least squares analysis of the power absorption curve). The rf magnetic field lines inside the cavity are concentric with the cylinder axis. H_{rf} is zero at the center and rises to a maximum value about three-quarters of the way out to the wall. At the wall, H_{rf} has a non-zero value. The beam experiences an oscillating rf magnetic field that is perpendicular to the static field H_o. The electric field and vector potential are directed parallel to the cavity axis and perpendicular to the faces. The beam hence experiences an oscillating rf electric field and vector potential that are parallel to the static magnetic field H_o.

A high-powered, continuous-wave microwave signal produced by a mechanically tuned magnetron is fed into the constant field region via a 1/2 inch, 50 ohm rigid coaxial transmission line and is inductively coupled to the cylindrical cavity. The coupler designed for this purpose is exposed in Fig. 2.

The hairpins consist of terminated 5/8 inch, 50 ohm rigid coaxial transmission lines. They produce an oscillating magnetic field at the beam which is, for the most part, at right angles to H_o, and is appropriate for stimulating π transitions. Fields oscillating in

phase and at a frequency equal to the transition frequency of interest are established in the two hairpins which are separated by a distance of six inches (center to center).

2. Radio-Frequency Equipment.

a. Transition Frequencies. Microwave signals at cesium transition frequencies are generated by a phase-locked, continuously operating klystron and fed to the separated hairpins as illustrated in Fig. 3. A very stable reference oscillator provides the fundamental comparison frequency. This comparison is made by a syncriminator which applies a correction voltage to the reflector of the klystron. A traveling-wave tube amplifies the klystron signal which is then divided, one-half being sent directly to one hairpin, and the other half being sent through a phase shifter and variable attenuator to the other hairpin. The attenuator allows one to equalize the rf field amplitudes in the two hairpins. The phase shifter provides a way of equalizing the phase of the signals reaching the hairpins by changing the electrical length of the transmission line leading to one of them. The two signals are judged to be in phase when a symmetrical Ramsey pattern is obtained; see Fig. 4.

Klystron frequencies are measured directly with a digital frequency counter which is capable of counting frequencies up to 12.4 GHz. Both the reference oscillator and the counter are referred to the same 100 kHz quartz crystal oscillator which is, in turn, continuously compared with the 60 kHz standard frequency broadcast by the National Bureau of Standards' station WWVB, Fort Collins, Colorado. Because

of the high stability of the 100 kHz reference, the precision of frequency measurements was determined by the uncertainty of ± 1 in the last place of the counter display.

b. Magnetron-Cavity Circuit. The circuit used to power the cavity is shown schematically in Fig. 5. The signal from an isolated, continously operating 100 watt magnetron can be fed either to the cavity or to a dummy load capable of absorbing 175 watts. Both input and return power are sampled with a 20 db dual directional coupler and measured with the same power meter. The magnetron frequency is measured directly with a digital frequency counter.

Insertion losses of all circuit components (including cables) were measured, so that the actual power absorbed by the cavity could be determined from power meter readings of input and return power. These measurements agreed with manufacturers' specifications when given.

4. Effective Fields of a TM_{010} Cavity. The effective fields experienced by an atomic beam that traverses an evacuated TM_{010} cylindrical cavity along a diameter midway between the ends are[16]

$$E = |E|e^{-i\omega t}, \quad B = i|B|e^{-i\omega t}, \quad A = -i|A|e^{-i\omega t}$$

where

$$|E|^2 = (0.455 \pm 0.023)\ E_o^2$$

$$|B|^2 = (0.212 \pm 0.009)\ E_o^2$$

$$|A|^2 = (0.455 \pm 0.023) \times (c/\omega)^2 E_o^2$$

and

$$E_o^2 = 203 \frac{PQ\nu_o}{\ell c^2} \quad .$$

P is the power absorbed in the cavity walls in erg/sec, Q is the unloaded Q, ν_o is the resonant frequency in Hz, ℓ is the length in cm, and c is the speed of light in vacuum. The numerical factors in the above equations were calculated by averaging the squares of the fields along a cavity diameter. The errors quoted are intended to account for the variation of the fields over the height of the beam (about 1/4 inch). When P is expressed in watts, ν_o in GHz, and ℓ in cm, the amplitude of the vector potential becomes

$$|A|^2 = 0.023 \frac{PQ}{\nu_o \ell}$$

and the electron relative mass shift is, for P = 1 W, Q = 4200, ν_o = 2.921 GHz, and ℓ = 1.91 cm,

$$\frac{\delta m}{m} = \frac{1}{2} \frac{e^2 |A|^2}{(mc^2)^2} = 4.03 \times 10^{-9} \frac{PQ}{\nu_o \ell}$$

$$\simeq 3 \times 10^{-6} \quad .$$

C. Experimental Procedure

At the start of each run, the magnetron was set for maximum output and tuned to the cavity resonant frequency. After several minutes the water-cooled cavity came to equilibrium, and the return power was steady and less than 1% of the input power. The signal observed at the detector for a constant static magnetic field, constant power input to the cavity, but varying hairpin frequency, is shown

in Fig. 4.

A measurement was then made of the position of the center of the central peak in the Ramsey pattern. This was done by averaging frequency readings taken at two or three positions symmetrically located on each side of the central peak. Hence, four or six frequency measurements, when averaged, gave one value for the center frequency. This procedure was performed ten times and the average of the ten center frequencies so measured was taken to be the best value for the transition frequency. Without changing the cavity input power, the transition frequency of the other member of the doublet was then determined in the same manner. The cavity power was then decreased, and, after equilibrium was achieved, the two frequencies were again measured. In this way the transition frequency was measured for five values of cavity power, including zero power. The five measurements of each transition frequency were then fit by a least squares procedure to a straight line with each point weighted in inverse proportion to its standard deviation; see Fig. 6.

IV. EXPERIMENTAL RESULTS

The results of twenty-seven measurements of ^{133}Cs hfs transition frequency shifts induced by the fields of a high-Q microwave cavity reveal no evidence for an electron mass shift. The measurements were sensitive enough to detect the Bloch-Siegert effect, which is more than two orders of magnitude smaller than the expected mass shift effect. The negative result is in agreement with the conclusion of Section II that the second-order effects of the plane-wave field cancel the hypothesized mass shift.

Figure 6 is a representative plot of transition frequency versus cavity power for one of the three field-independent doublets studied and indicates how well the data fit a straight line dependence. The effective cavity power is obtained by considering (a) the calibration of the absorbed cavity power versus the power meter reading, (b) the factor arising from the cavity filling only part of the measuring region, and (c) the characteristics of the method of sensing a change in energy in the region between the separated transition loops.

Table II summarizes all experimental results. Each measurement listed is the average for four or five runs; the errors given represent the repeatability of the shifts and the uncertainties associated with Q, with the power P, and with the averages of the cavity fields over the beam height. The designations a_1, a_2, etc., refer to the notation of Table I and Fig. 1. The observed shifts, S_{obs}, are given in both Hz/W and Hz/G^2 for comparison with the expected mass-shift effect, S_{ms}, and

Bloch-Siegert effect, S_{BS}. In addition to the discrepancy in absolute size (more than two orders of magnitude) between the observed shifts and those expected due to an electron mass shift, there is also a striking discrepancy in the relative size of the shifts of the two 2100 G transitions c_1 and c_2. If these shifts were due to an increase in the electron mass, the two should be equal (to within a few percent), whereas they differ by a factor of about 3.7.

On the other hand, there is good agreement between the six observed shifts and those expected on the basis of a many-level Bloch-Siegert effect. This effect amounts to a shift in the maximum transition probability (i.e., the central peak of the Ramsey pattern) due to the presence of a non-resonant perturbation. Evidently, the rf magnetic field in the cavity has been slightly overestimated, causing the calculated Bloch-Siegert shifts to be somewhat larger than the listed measurements. The relative sizes of the six measurements agree completely, within experimental error, with the calculated Bloch-Siegert shifts.

An oscillating magnetic field H_{rf}, oriented at right angles to a uniform C-field H_o, shifts a given magnetic dipole transition frequency f by[17]

$$\Delta f = \left(g_J \frac{\mu_o}{h} \frac{H_{rf}}{2}\right)^2 \sum_j \sum_i \left\{ \frac{|\langle i|J_x|1\rangle|^2}{\left(\frac{E_i - E_1}{h} - \nu_j\right)} + \frac{|\langle 2|J_x|i\rangle|^2}{\left(\frac{E_2 - E_i}{h} - \nu_j\right)} \right\} \tag{14}$$

where $(E_2 - E_1)/h$ is the transition frequency under study. The index j takes on two values corresponding to $\nu_j = \pm \nu_o$, the frequency of the non-resonant perturbation. The index i runs through all the states

that that can be reached by a π-type transition from either the inital or the final state. This many-level Bloch-Siegert effect is seen to be proportional to the square of the rf magnetic field and hence is a linear function of power.

Perhaps the quickest way to test whether one is observing the Bloch-Siegert effect or the mass-shift effect is to choose a cavity mode for which the mass shift theory predicts large, positive, and equal frequency shifts for the two members of a π doublet, while the expected Bloch-Siegert shifts are small, negative, and unequal. Such is the case for the 2100 G doublet when the cavity frequency is 7930 MHz, and H_{rf} is perpendicular to H_o. Seven runs were made at this frequency using a TM_{210} cavity powered by a mechanically tuned magnetron. Figure 7 is a plot of transition frequency versus power for one such run. The frequency shifts are clearly negative and unequal. The results of these runs reinforce the conclusion drawn from Table II; namely, that all shifts observed can be interpreted as Bloch-Siegert shifts.

V. CONCLUSION. WHY THE MASS SHIFT EFFECT WAS NOT OBSERVED

Arguments similar to those given in Section II-D can be invoked to explain the negative result. There are three ways in which the constant term $e^2A^2_{rot}$ appearing in Eq. (4) may be handled: (i) combine $e^2A^2_{rot}$ with $(mc^2)^2$ to get a renormalized mass as was done in Section II; (ii) combine $e^2A^2_{rot}$ with $W = E - mc^2$ and get the same shift for all energy levels; or (iii) leave the term in the equation until after the non-relativistic approximation has been obtained, treat it by perturbation theory, and get an equal shift of all energy levels. Alternatives (ii) and (iii) are equivalent to order $1/m^2$, i.e., when the relativistic term $\frac{1}{2mc^2}(W - e\phi)^2$ is neglected.

Although the discussion of Section II was concerned with a hydrogen-like atom in a <u>circularly</u> polarized plane wave field, the oscillating fields experienced by a beam atom traversing a diameter of a TM_{010} cavity are roughly similar to those of a <u>linearly</u> polarized plane wave. Such a wave can be represented by

$$\vec{A} = \hat{\varepsilon} a e^{i(kx - \omega t)}$$

$$A^2 = \frac{a^2}{2}(1 + \cos 2(kx - \omega t))$$

where $\hat{\varepsilon}$ is the (real) polarization vector. If the $e^2A^2_{rot}$ term is carried through to the non-relativistic approximation, it becomes

$$\frac{e^2A^2_{rot}}{2mc^2} = \frac{e^2a^2}{4mc^2} + \frac{e^2a^2}{8mc^2}(e^{2ikx} + e^{-2ikx})$$

where the $e^{\pm 2i\omega t}$ factors in the cosine have been set to their zeroth order values, namely, unity. When the previously neglected $\frac{-e}{mc}\vec{A}_{rot}\cdot\vec{p}$ term is again treated in second-order perturbation theory and the

$e^2A^2_{rot}/(2mc^2)$ term is treated in first-order perturbation theory one obtains, with the aid of Eq. (12),

$$-\frac{e}{2mc}\vec{A}_{rot}\cdot\vec{p} \rightarrow -\frac{e^2a^2}{2mc^2}$$

and

$$\frac{e^2A^2_{rot}}{2mc^2} \rightarrow \frac{e^2a^2}{4mc^2} + \frac{e^2a^2}{8mc^2} \times 2 = \frac{e^2a^2}{2mc^2} \quad .$$

Therefore, the first-order energy shift due to the mass renormalization term is again exactly canceled by the second-order energy shift due to the $\vec{A}_{rot}\cdot\vec{p}$ term. In the light of the negative experimental results, it appears that the proper way to treat the $e^2A^2_{rot}$ term is by perturbation theory, and not to consider it as an electron mass renormalization.

ACKNOWLEDGMENTS

We acknowledge Professors Charles Schwartz, P. G. H. Sandars, and W. A. Nierenberg, who each suggested independently that the mass-shift effect probably would not occur for hydrogen-like atoms because the $e^2A_{rot}^2$ term might be canceled by the $\vec{A}_{rot}\cdot\vec{p}$ term in second-order perturbation theory.

FOOTNOTES

*This paper is based on a thesis submitted by J. Richard Mowat to the Graduate Division, University of California, Berkeley, 1969, in partial fulfillment of the requirements for the degree of Doctor of Philosophy; the work was supported by the U. S. Atomic Energy Commission and has been reported in UCRL-19245, August 1969 (unpublished).

†Present Address: Department of Physics, Brandeis University, Waltham, Massachusetts 02154.

[1] H. R. Reiss and J. H. Eberly, Phys. Rev. 151, 1058 (1966).

[2] N. D. Sengupta, Calcutta Mathematical Society Bulletin 44, 175 (1952).

[3] E. S. Sarachik, National Aeronautics and Space Administration Report NASA-TN-D5205 (unpublished), May 1969.

[4] H. R. Reiss, Phys. Rev. Letters 17, 1162 (1966).

[5] J. R. Mowat, C. E. Johnson, V. J. Ehlers, and H. A. Shugart, Bull. Am. Phys. Soc. 14, 524 (1969).

[6] H. A. Bethe and E. E. Salpeter, Quantum Mechanics of One and Two-Electron Atoms (Springer-Verlag, Berlin, 1957), p. 56.

[7] J. D. Bjorken and S. D. Drell, Relativistic Quantum Mechanics (McGraw-Hill, New York, 1964), p. 51.

[8] G. Breit and I. I. Rabi, Phys. Rev. 38, 2082 (1931).

[9] I. I. Rabi, Phys. Rev. 51, 652 (1937).

[10] F. Bloch and A. Siegert, Phys. Rev. 57, 522 (1940).

[11] See reference 6, p. 252 and p. 279.

[12] G. Breit, Phys. Rev. 42, 348 (1932).

[13] H. Kopfermann, Nuclear Moments (Academic Press, New York, 1958), p. 136.

[14] J. R. Zacharias, Phys. Rev. 61, 270 (1942); P. A. Vanden Bout, V. J. Ehlers, W. A. Nierenberg, and H. A. Shugart, Phys. Rev. 158, 1078 (1967).

[15] N. F. Ramsey, Phys. Rev. 78, 695 (1950); M. Mizushima, Phys. Rev. 133A, 414 (1964).

[16] J. D. Jackson, Classical Electrodynamics (John Wiley, New York, 1962), p. 254.

[17] N. F. Ramsey, Phys. Rev. 100, 1191 (1955).

Table I. ^{133}Cs field-independent $\Delta F = 1$ transitions. The designations a, b, or c refer to the transitions labelled in Fig. 1; these are the transitions for which frequency shifts were observed.

Designation	Transition (F,m_F)	Type	Field-Independent Parameters Field (Gauss)	Frequency (MHz)
	$(4,0) \leftrightarrow (3,0)$	σ	0	9192.631770
a_1	$(4,-1) \leftrightarrow (3,0)$	π	416	9119.6
a_2	$(4,0) \leftrightarrow (3,-1)$	π	417	9119.1
	$(4,-1) \leftrightarrow (3,-1)$	σ	820	8900.7
b_1	$(4,-2) \leftrightarrow (3,-1)$	π	1252	8509.5
b_2	$(4,-1) \leftrightarrow (3,-2)$	π	1253	8508.1
	$(4,-2) \leftrightarrow (3,-2)$	σ	1640	7961.0
c_1	$(4,-3) \leftrightarrow (3,-2)$	π	2104	7115.3
c_2	$(4,-2) \leftrightarrow (3,-3)$	π	2105	7112.9
	$(4,-3) \leftrightarrow (3,-3)$	σ	2460	6080.4

Table II. Comparison of observed shifts (S_{obs}) with predicted shifts for the mass-shift effect (S_{ms}) and the Bloch-Siegert effect (S_{BS}).

Transition	Frequency (MHz)	S_{ms} (Hz/watt)	S_{obs} (Hz/watt)	S_{obs} (Hz/Gauss^2)	S_{BS} (Hz/Gauss^2)
a_1	9119.6	$55 \pm 4 \times 10^3$	154 ±9	50 ±3	60
a_2	9119.1	55 ±4	154 ±15	50 ±3	62
b_1	8509.5	52 ±4	172 ±9	56 ±3	61
b_2	8508.1	52 ±4	191 ±7	62 ±4	72
c_1	7115.3	43 ±3	94 ±6	30 ±2	38
c_2	7112.9	43 ±3	349 ±46	113 ±8	150

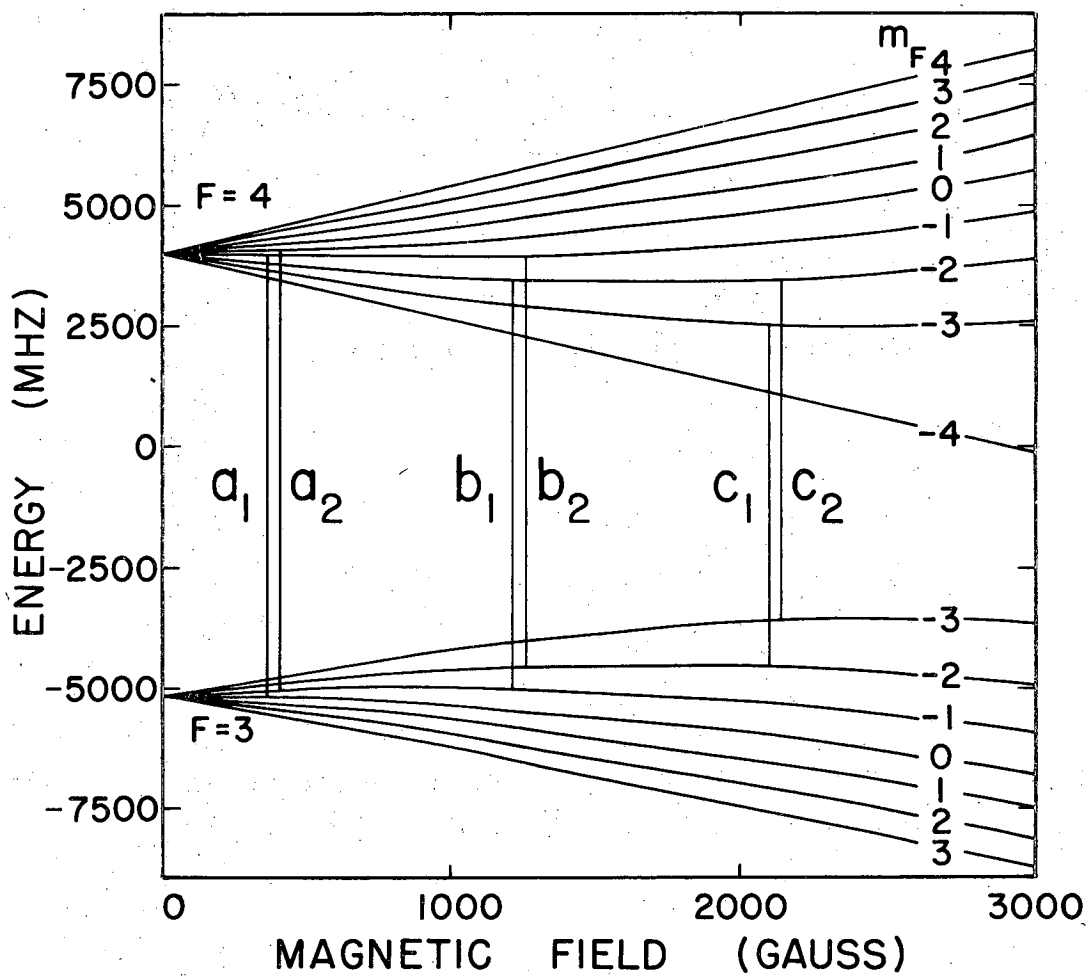

XBL 6910 - 5772

Fig. 1. Breit-Rabi diagram for ^{133}Cs. The three $\Delta F=1$ $\Delta m_F=\pm 1$ field-independent doublet transitions are shown; the labels correspond to the notation in Table I.

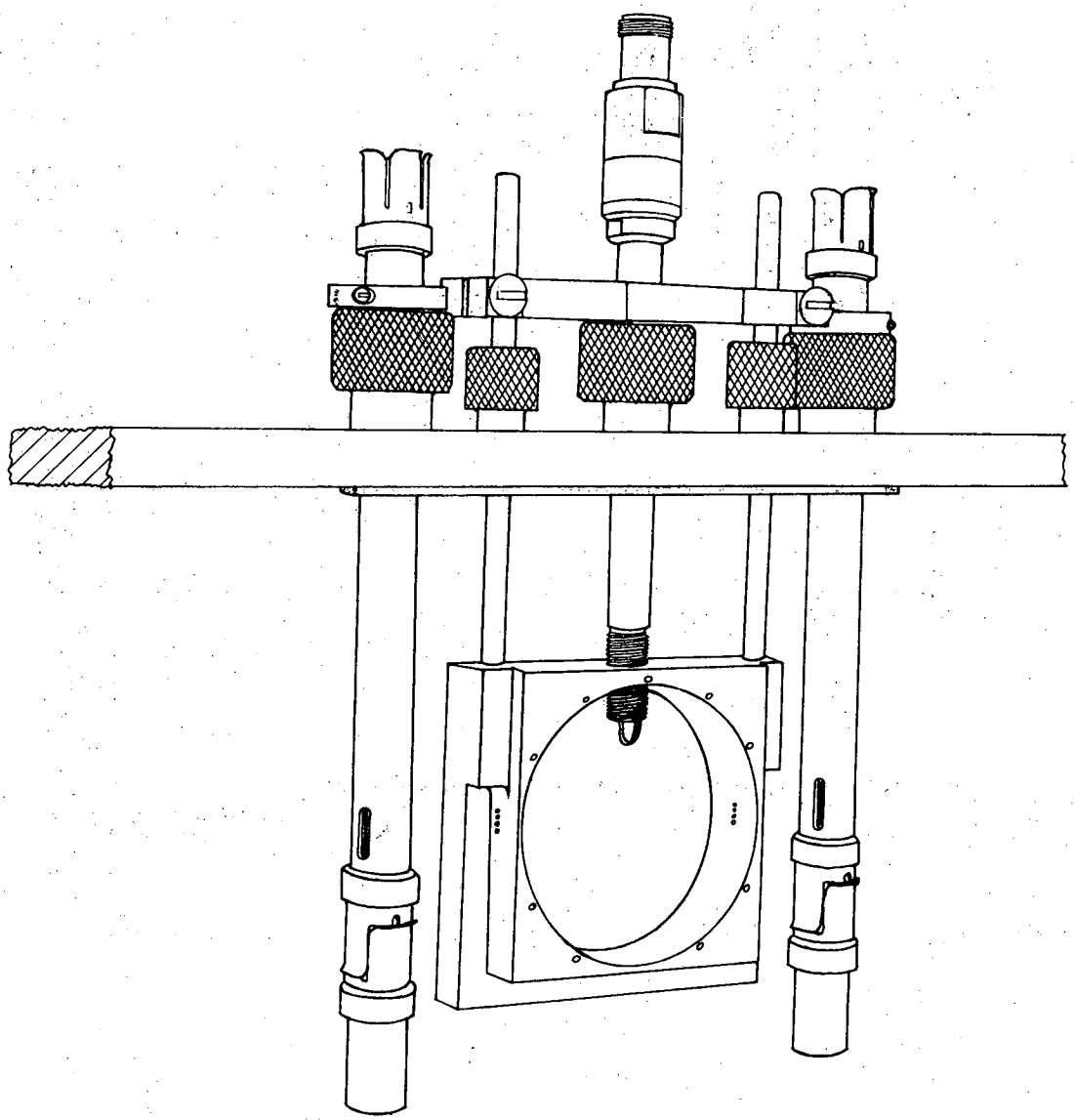

XBL 6910-5773

Fig. 2. Sketch of the microwave cavity and the two separated transition hairpins.

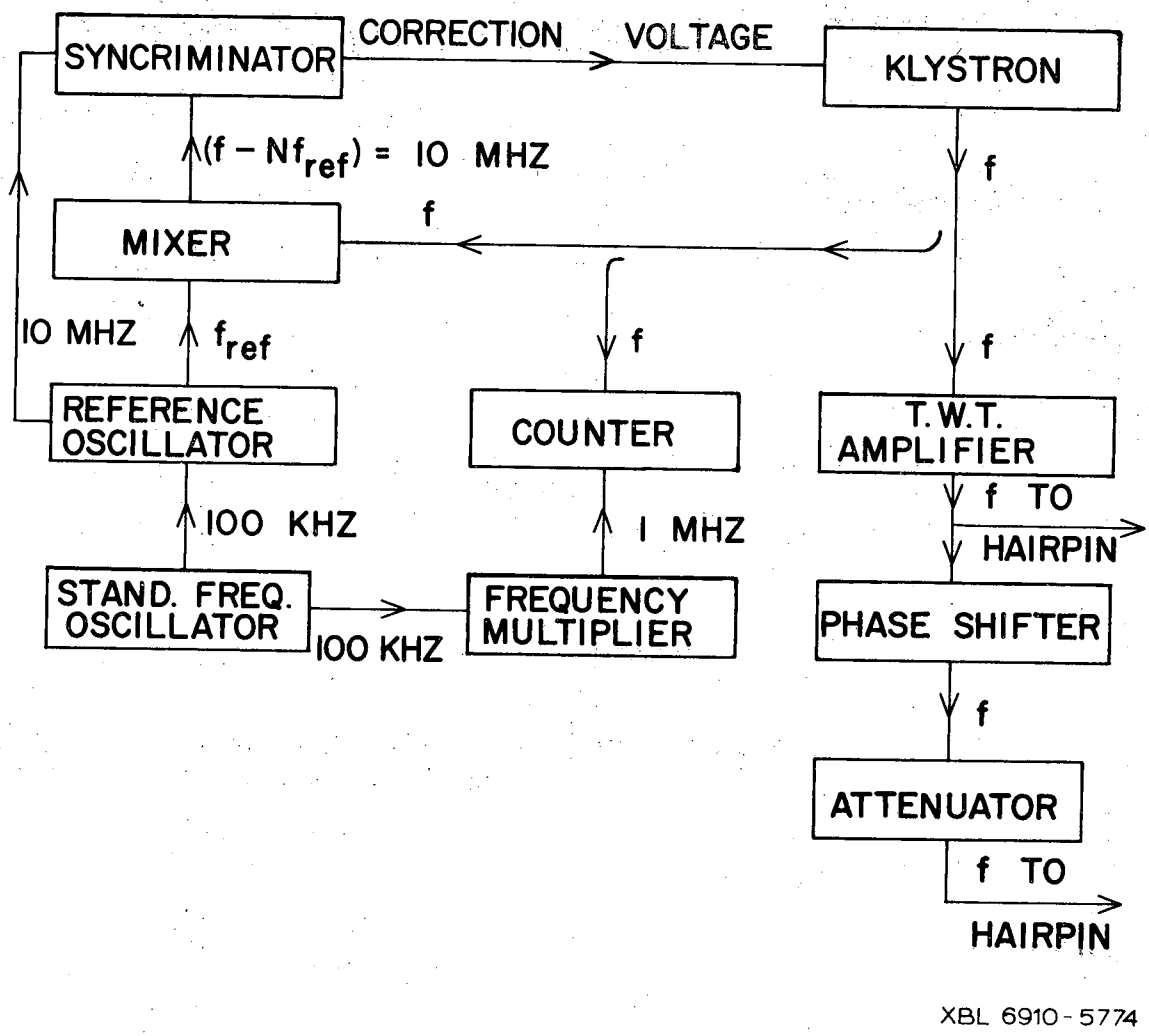

Fig. 3. Radiofrequency arrangement for driving the separated oscillating field hairpins.

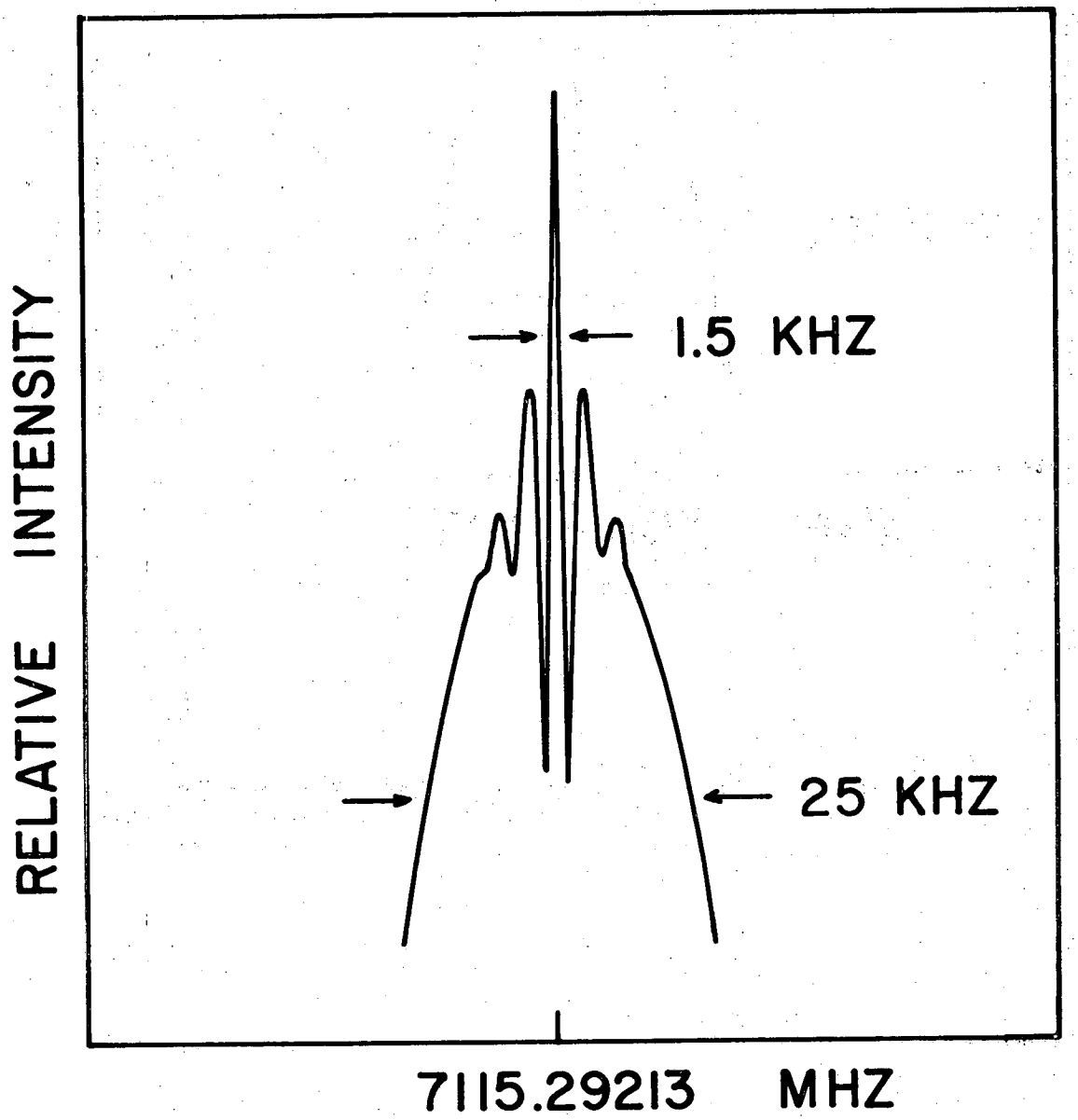

XBL 6910-5775

Fig. 4. Representative Ramsey pattern used in measurements of frequency shifts.

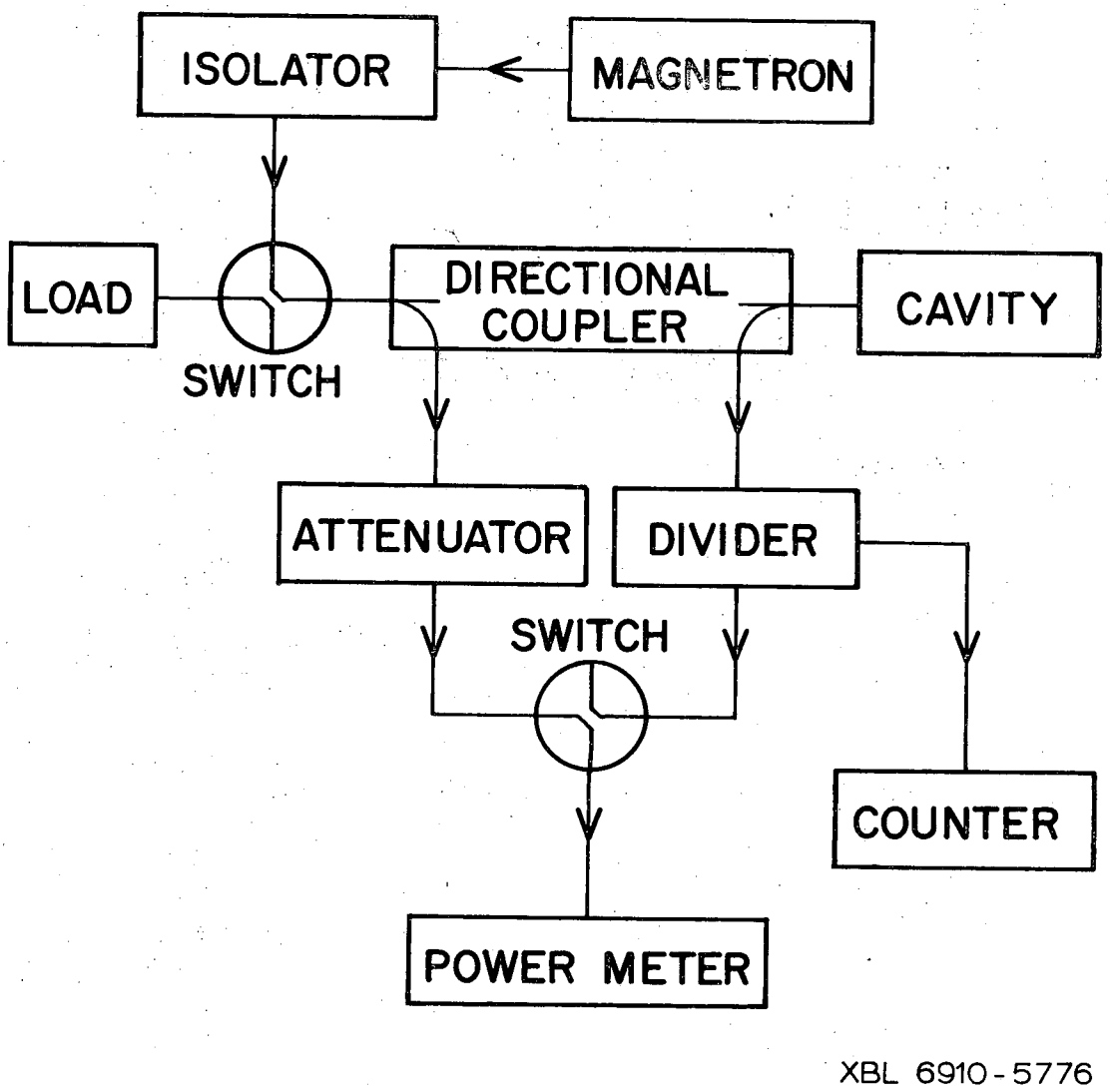

Fig. 5. Circuit used to power the microwave cavity.

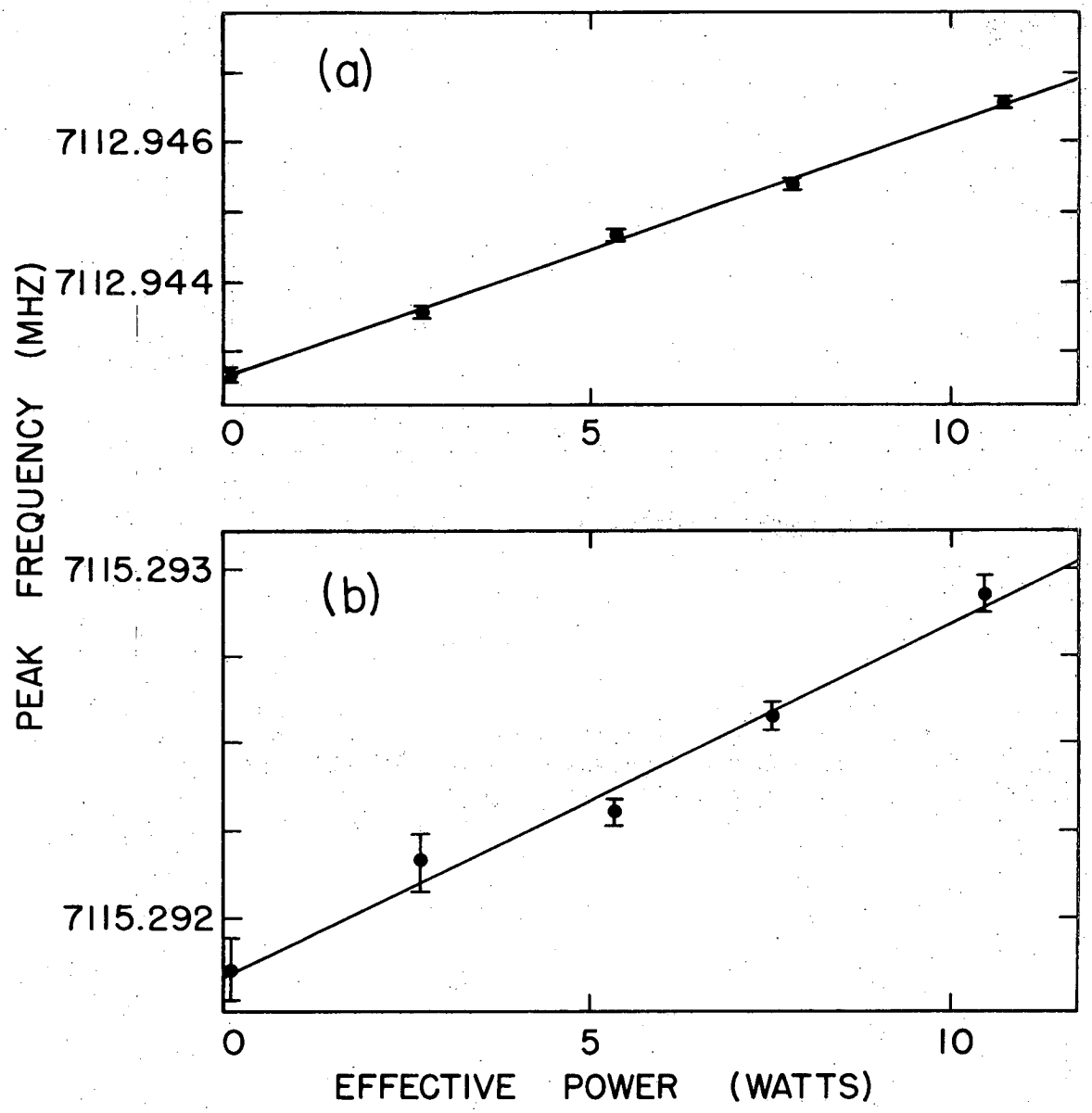

XBL 6910-5777

Fig. 6. Transition frequency versus effective rf cavity power for the 2100-gauss doublet, using a cavity frequency of 2921 MHz. Curve (a) is the (4,-2)↔(3,-3) transition and curve (b) is the (4,-3)↔(3,-2) transition.

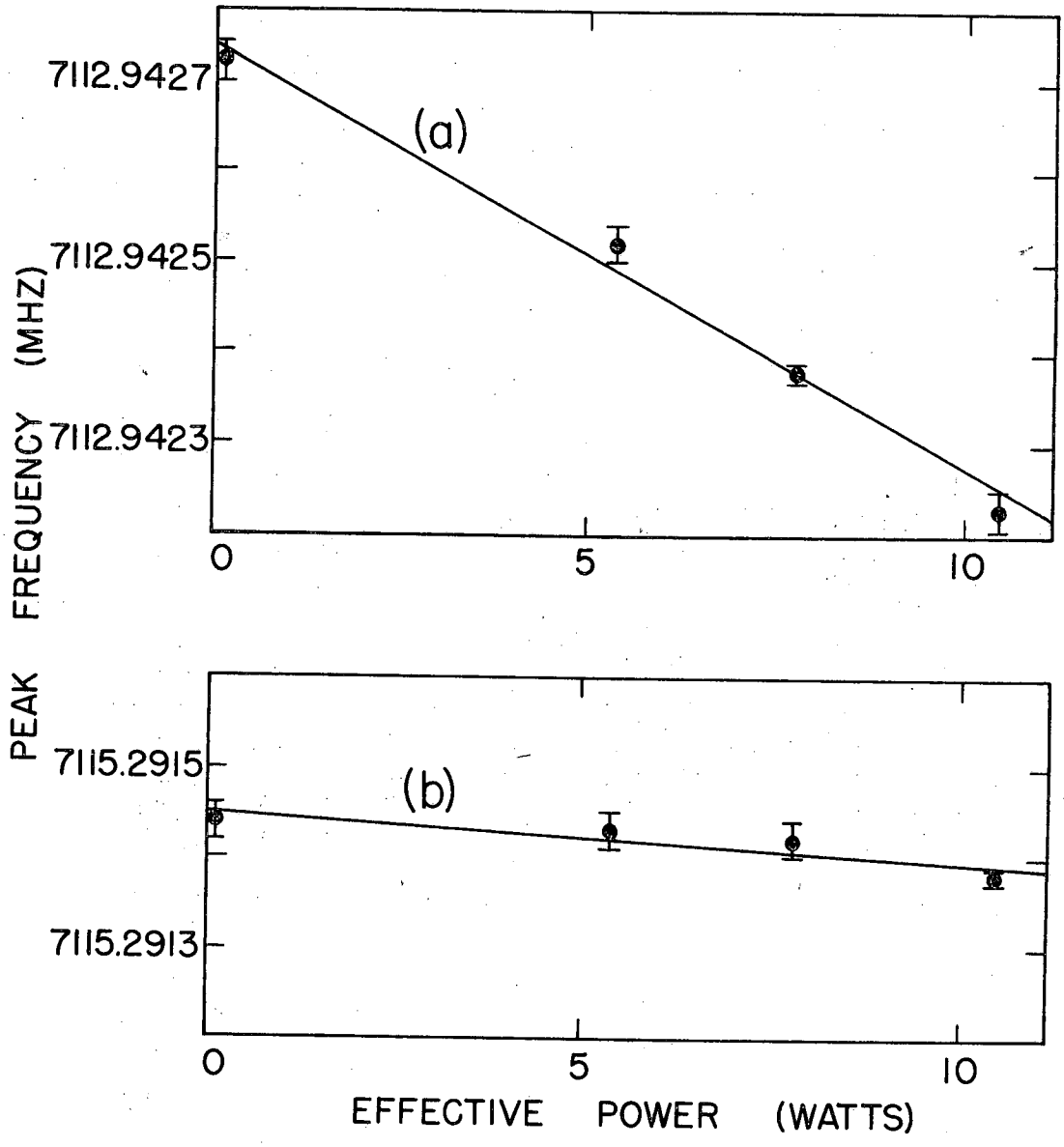

XBL 6910-5778

Fig. 7. Transition frequency versus effective rf cavity power for the 2100-gauss doublet, using a cavity frequency of 7930 MHz. Curve (a) is the (4,-2)↔(3,-3) transition and curve (b) is the (4,-3)↔(3,-2) transition.

LEGAL NOTICE

This report was prepared as an account of Government sponsored work. Neither the United States, nor the Commission, nor any person acting on behalf of the Commission:

A. Makes any warranty or representation, expressed or implied, with respect to the accuracy, completeness, or usefulness of the information contained in this report, or that the use of any information, apparatus, method, or process disclosed in this report may not infringe privately owned rights; or

B. Assumes any liabilities with respect to the use of, or for damages resulting from the use of any information, apparatus, method, or process disclosed in this report.

As used in the above, "person acting on behalf of the Commission" includes any employee or contractor of the Commission, or employee of such contractor, to the extent that such employee or contractor of the Commission, or employee of such contractor prepares, disseminates, or provides access to, any information pursuant to his employment or contract with the Commission, or his employment with such contractor.

TECHNICAL INFORMATION DIVISION
LAWRENCE RADIATION LABORATORY
UNIVERSITY OF CALIFORNIA
BERKELEY, CALIFORNIA 94720